

Measurement of NO_x Fluxes from a Tall Tower in Central London, UK and Comparison with Emissions Inventories

James D. Lee,^{*,‡,†} Carole Helffer,[§] Ruth M. Purvis,^{‡,†} Sean D. Beevers,[‡] David C. Carslaw,[‡] Alastair C. Lewis,[†] Sarah J. Möller,^{‡,†} Anja Tremper,[‡] Adam Vaughan,[‡] and Eiko G. Nemitz[§]

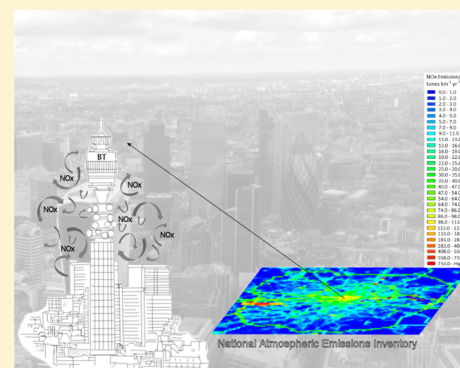
[†]National Centre for Atmospheric Science and [‡]Department of Chemistry, University of York, York YO10 5DD, U.K.

[§]Centre for Ecology and Hydrology (Edinburgh Research Station), Penicuik EH26 0QB, U.K.

[‡]Environmental Research Group, King's College London, Fourth Floor, Franklin Wilkins Building, 150 Stamford Street, London WC2R 2LS, U.K.

S Supporting Information

ABSTRACT: Direct measurements of NO_x concentration and flux were made from a tall tower in central London, UK as part of the Clean Air for London (ClearFlo) project. Fast time resolution (10 Hz) NO and NO₂ concentrations were measured and combined with fast vertical wind measurements to provide top-down flux estimates using the eddy covariance technique. Measured NO_x fluxes were usually positive and ranged from close to zero at night to 2000–8000 ng m⁻² s⁻¹ during the day. Peak fluxes were usually observed in the morning, coincident with the maximum traffic flow. Measurements of the NO_x flux have been scaled and compared to the UK National Atmospheric Emissions Inventory (NAEI) estimate of NO_x emission for the measurement footprint. The measurements are on average 80% higher than the NAEI emission inventory for all of London. Observations made in westerly airflow (from parts of London where traffic is a smaller fraction of the NO_x source) showed a better agreement on average with the inventory. The observations suggest that the emissions inventory is poorest at estimating NO_x when traffic is the dominant source, in this case from an easterly direction from the BT Tower. Agreement between the measurements and the London Atmospheric Emissions Inventory (LAEI) are better, due to the more explicit treatment of traffic flow by this more detailed inventory. The flux observations support previous tailpipe observations of higher NO_x emitted from the London vehicle diesel fleet than is represented in the NAEI or predicted for several EURO emission control technologies. Higher-than-anticipated vehicle NO_x is likely responsible for the significant discrepancies that exist in London between observed NO_x and long-term NO_x projections.



INTRODUCTION

The oxides of nitrogen NO_x (defined as the sum of NO and NO₂), are emitted as a consequence of most combustion processes. The majority of NO_x is emitted as NO, which is rapidly oxidized to NO₂ upon reaction with ozone (O₃), with the reverse of this process being caused by the action of sunlight on NO₂ to form NO and O₃. NO₂ is known to have significant direct health effects on humans. At high concentrations it causes inflammation of the airways, and long-term exposure may affect lung function and enhance the response to allergens.^{1,2} In addition, NO_x contributes to the formation of O₃ and secondary particles through a series of photochemical reactions.³ As a result of this, NO₂ is included in a series of air pollutants identified as part of the EU Air Quality Directive (AQD, 2008)⁴ which sets limit values for hourly and annual mean exposure. It has been shown by measurements and models that the annual mean limit value of 40 μg m⁻³ continues to be exceeded in many urban centers throughout the UK,⁵ including London. Measures are in place to control the emissions of nitrogen oxides, and UK emissions are projected

to decline by about 35% between 2010 and 2020.⁶ However, it is known that ambient NO₂ concentrations do not respond linearly to reductions in the concentration of NO_x (e.g., Derwent et al.⁷), mainly because of the chemical coupling of ozone (O₃) and NO_x under ambient conditions.⁸ In addition, changes in diesel emission control technology have led to increases in directly emitted NO₂.⁹ Trends in ambient concentrations of NO_x and NO₂ in the UK have generally shown a decrease in concentration from 1996 to 2002, followed by a period of more stable concentrations from 2004–2012.¹⁰ This is not in line with the expected decrease suggested by the UK emission factors.¹¹

Air pollutant emission inventories provide input data for air pollution models, which in turn are used for predicting current and future air pollution. This is typically done using a “bottom

Received: October 8, 2014

Revised: December 11, 2014

Accepted: December 12, 2014

Published: December 12, 2014

up” approach involving estimated emissions from different source sectors to produce yearly emission estimates. However, it is known that this method can contain large uncertainties, with the errors propagating through into errors in air pollution models.¹² Evaluation of emission inventories can be carried out by comparing air quality model predictions (using inputs from the inventory) to observed concentrations,^{13,14} however this method does not provide a direct comparison with the emission rate as it requires knowledge of other parameters such as chemistry and meteorology. The eddy covariance technique provides a direct measurement of the flux to the atmosphere of a particular pollutant, thus providing a “top down” approach to quantifying emissions.¹⁵ Flux measurements also provide information on both spatial and temporal change in emissions from a calculated flux footprint, giving insight into controls and sources. The majority of eddy covariance measurements made to date have concentrated on fluxes of greenhouse gases (CO₂, CH₄, and N₂O)^{16,17} and volatile organic compounds (VOCs),^{18–20} largely from biogenic sources. Some eddy covariance NO_x flux measurements have been made and have typically focused on emissions from soils,²¹ forests,^{22–24} or snow.^{25,26} Recently, however, it has been shown that this method can be extended to the urban canopy for CO₂^{27–29} and VOCs,^{30–32} with one study of urban NO_x.³³

In this study, we use the eddy covariance technique to directly measure the flux of NO and NO₂ from a tall tower (190 m) in central London as part of the Clean Air for London (ClearfLo) project.³⁴ The results are compared to local traffic flow, and a flux footprint is calculated to allow comparison with two emission inventories, one for the whole of the UK and one specific to London.

EXPERIMENTAL SECTION

Measurement Site. Measurements were made during June–August 2012 and March–April 2013 from the top of the BT Tower, a 190-m-tall telecommunications tower situated in central London, UK (51°31'17.4"N, 0°8'20.04"W). Mean building height is 8.8 ± 3.0 m within 1–10 km of the tower and 5.6 ± 1.8 m for suburban London beyond this.^{30,35} The area surrounding the tower is dominated by roads and commercial/residential buildings, but also includes some urban parkland and pervious ground. A map of the location of the tower within London is shown in the Supporting Information (SI) (Figure S1). The gas inlet and ultrasonic anemometer were attached to a mast that extended ~3 m above the top of the tower. Air was pumped down a ~40-m Teflon tube (1/2 in. OD) at a flow rate of ~30 L min⁻¹ to the gas instruments, which were housed in a room inside the tower.

The most prevalent wind direction during the summer 2012 measurement period was the SW sector (~50% of the time), with other wind sectors split approximately equally. Wind speed was 6.7 m s⁻¹ on average, with the highest wind speeds measured when the wind was from a NW direction. Average temperature was 15.1 ± 4.3 °C. During the March–April 2013 measurement period, the most prevalent wind direction was between 0–90° (50%), again with other directions split approximately equally. Wind speed was higher than that of summer 2012, being 8.8 m s⁻¹ on average, with the highest wind speed when the wind was from the SW direction. As expected, average temperature was lower than that of the summer 2012 period, being 9.7 ± 2.4 °C.

NO_x Measurements. Measurements of NO were made using an Ecophysics 780TR instrument, which uses the

chemiluminescence technique.^{36,37} NO₂ was quantified in a second identical NO instrument by initial photolytic conversion to NO using blue light LED diodes centered at 395 nm. The 395-nm wavelength has a specific affinity for NO₂ photolytic conversion to NO, giving high analyte selectivity within the channel,³⁸ and there is a low probability of other species such as nitrous acid (HONO) being photolyzed. The diode-based converter also has a very low residence time for the air sample (<0.1 s) which allows 10 Hz measurements of NO₂ to be made. The NO instruments were calibrated every 36 h by addition of a known amount of NO to the sample line, made by diluting a gas standard (5 ppm of NO in N₂, BOC – traceable to NPL scale) in NO_x free air (Ecophysics PAG003). The conversion efficiency of the NO₂ converter was also measured during each calibration by gas-phase titration of the known NO upon addition of O₃, with typical conversion efficiencies being 30–35%. It is estimated that the total error (including accuracy and precision) is around 10% for NO and 15% for NO₂ at 10 ppbV.

Meteorology Measurements. Fast (20 Hz), 3-dimensional wind vectors and sonic temperature were measured from next to the sample line inlet by a Gill Instruments R3-50 ultrasonic anemometer. The data were logged, along with that from the NO_x instrument, using a custom National Instruments LabView program. The boundary layer height was measured using a HALO Photonic Doppler LiDAR instrument.³⁹

Flux Calculations and Uncertainties. NO and NO₂ fluxes (F_{NO} and F_{NO_2}) were calculated using eqs 1 and 2.

$$F_{\text{NO}} = \frac{w' C'_{\text{NO}}}{S_{\text{NO}} V_{\text{mol}}} \quad (1)$$

$$F_{\text{NO}_2} = \frac{1}{\alpha V_{\text{mol}}} \left\{ \frac{w' C'_{\text{NO}_2}}{S_{\text{NO}_2}} - \frac{w' C'_{\text{NO}}}{S_{\text{NO}}} \right\} \quad (2)$$

C_i is the number of instrument counts (in Hz) and S_i is the associated instrument sensitivity (in Hz ppb⁻¹) for species i (NO and NO₂). V_{mol} is the molar volume (calculated for each individual point), α is the photolytic conversion efficiency of NO₂ to NO, and w is the vertical wind component measured by the ultrasonic anemometer. A “prime” symbol represents an instantaneous deviation from the mean, and a horizontal bar denotes the covariance of 2 scalars.

Processed data were filtered using a three-step quality assurance algorithm whereby data were deemed of satisfactory quality if the following conditions were met: The level of turbulence was sufficient, i.e. locally derived friction velocity $u^* \geq 0.2 \text{ m s}^{-1}$ (<5% of the data is rejected due to this parameter). The number of spikes in w , NO, and NO₂ did not exceed 1% of total in each half-hourly averaging period. The stationarity test described by Foken et al.,^{40,41} which requires the flux for the complete averaging interval (here 30 min) to be within 30% of the fluxes calculated for the subintervals (6 × 5 min), was satisfied.

Total measurement uncertainty, i.e. the sum of total random and systematic uncertainties, was estimated using the 24-h differencing method⁴² which assumes that the difference between pairs of observations taken exactly 24 h apart under similar meteorological conditions (air temperature, wind speed, and direction) is mainly attributable to stochastic factors. Using multiple pairs of observations, the standard deviation of the random error can be calculated from eq 3.

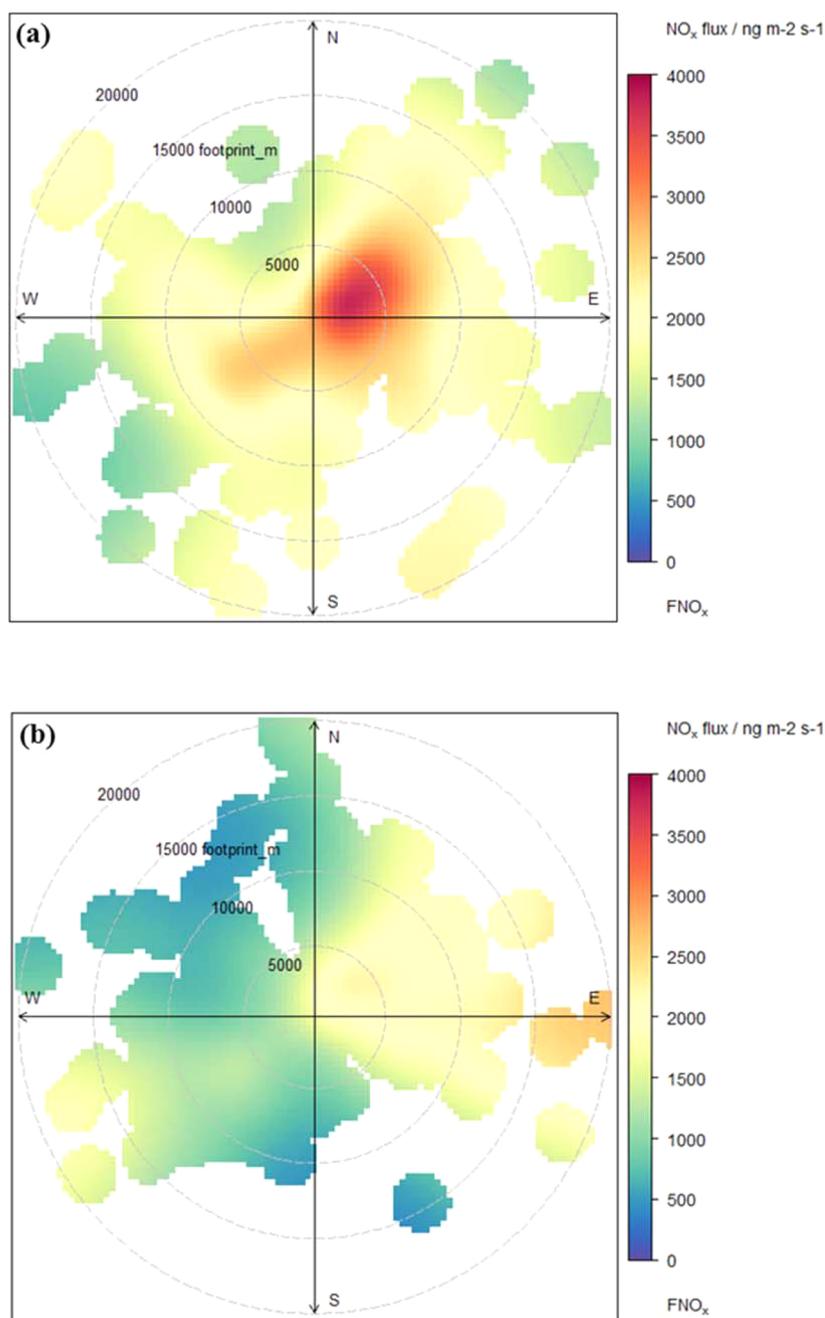


Figure 1. Wind-sector dependence of the NO_x flux for all data averaged during (a) daytime (05:00–19:00) and (b) nighttime (20:00–04:00). The radial axis shows the calculated flux footprint in meters for each measurement.

$$\sigma = \frac{\sigma(x_{1,t} - x_{2,t})}{\sqrt{2}} \tag{3}$$

The environmental conditions were deemed similar if air temperatures diverged by less than 3 °C, wind speed diverged by less than 2 m s⁻¹, and wind directions originated from the same quadrant.

Causes of systematic uncertainties are varied and include calibration procedures, instrumentation limitations, or data processing artifacts. Unlike random uncertainties, systematic errors can be minimized by careful data processing and correction.

Successive calibration events were linearly interpolated over time, canceling out errors due to calibration drifts provided that the drift was linear over time.

To estimate potential turbulence attenuation in the sampling line, which can lead to underestimation of the actual flux, fluxes of CO₂ measured using by a Picarro G2301-f sampling off the same line as the NO and NO₂ analyzers were compared with fluxes measured by a Licor 7500 open-path analyzer mounted near the ultrasonic anemometer. The underlying assumption is that turbulence attenuation and molecular interactions with the sampling tube are comparable for CO₂, NO, and NO₂ molecules. Rather than correct for attenuation, this systematic uncertainty was added to the estimated stochastic component and presented as confidence interval in what follows.

Flux Footprint. To carry out meaningful interpretation of the data, it is necessary to calculate the flux footprint of the measurement. It is not possible to get footprint models to fully account for the spatial variability of building heights, topography, and surface heat flux from an urban environment. In this case, the Kormann and Meixner⁴³ footprint model (K–M model) was applied, which accounts for non-neutral stratification but assumes homogeneous surfaces. The aerodynamic roughness length for momentum was assumed to be 1 m as used in previous BT Tower flux studies.³⁵ The sample height for the BT Tower was 190 m. The K–M model was used to estimate the flux footprint on a half-hourly time base. A Microsoft Excel tool (based on the K–M model) calculated the distance from the measurement point from which a set percentage of the measured flux is emitted. Figure S4 in the SI shows a histogram of the calculated footprints for 50%, 70%, and 90% of the flux for the measurement period. The analysis here uses the footprint from which 90% of the flux is predicted to originate, which shows a range of 150–19 980 m, with a median of 4695 m.

RESULTS AND DISCUSSION

Measurements of the NO_x flux were made during two time periods, June–August 2012 (36 days) and March–April 2013 (28 days). Downtime was due mainly to instrument failure of both the fast NO_x instrument and 3-D sonic anemometer, as well as a failure in the sample pump. Despite this, data coverage on the days when measurements was taken was 61%, meaning the data set provides a unique opportunity to examine the diurnal and seasonal behavior of NO_x fluxes from central London.

The full time series of data is shown in the SI Figure S2, with NO_x concentrations averaged to the 30-min flux averaging time. Typically NO concentrations vary from close to zero at night to a maximum of 10–100 μg m⁻³ during the day, whereas NO₂ ranges from 5–80 μg m⁻³. Also shown in SI Figure S2 is the time series of NO and NO₂ from an urban background site in at North Kensington, London, which is approximately 5 km west of the BT Tower.⁴⁴ These data show a trend similar to that of the BT Tower for most of the time, although at generally higher levels. A regression analysis of the two data sets (BT Tower and North Kensington, shown in SI Figure S3), shows North Kensington data being on average 10% higher for NO and 6% higher for total NO_x (*R*² of 0.65 and 0.58, respectively). This result gives confidence that, at least for total NO_x, the BT Tower site is representative of the wider London area.

Random uncertainties (1 σ) obtained by 24-h differencing were 441 ng m⁻² s⁻¹ for *F*_{NO}, 475 ng m⁻² s⁻¹ for *F*_{NO₂}, and 510 ng m⁻² s⁻¹ for *F*_{NO_x} (*F*_{NO} + *F*_{NO₂}); residual systematic uncertainties were estimated at 15% of the measured flux. Maximum NO_x fluxes are measured during the daytime, with values from 2000 ± 741 to 5000 ± 1191 ng m⁻² s⁻¹ for NO and 2000 ± 775 to 12 000 ± 2275 ng m⁻² s⁻¹ for NO₂. Measured fluxes are usually positive, demonstrating, as expected, that NO_x emission dominates over deposition in this urban environment and that it is likely to be dominated by anthropogenic emissions. NO_x can be lost to the surface by dry deposition,⁴⁵ and assuming a deposition velocity of 0.1 cm⁻¹ and a NO_x concentration of 50 μg m⁻³, then the downward flux can be estimated to be in the region of 100 ng m⁻² s⁻¹, which is more than an order of magnitude smaller than the observed values. NO and NO₂ fluxes show a distinct diurnal profile. NO

flux is close to zero at night (although still positive), with a rise starting at 05:00 to a peak of 1800–1900 ng m⁻² s⁻¹ between 08:00 and 12:00. The NO flux then usually starts to decrease throughout the rest of the day and into the night, reaching the nighttime value of 100–200 ng m⁻² s⁻¹ at around 20:00. NO₂ flux also typically shows a diurnal profile with 500–1000 ng m⁻² s⁻¹ measured at night followed by a rise to 2200–2300 ng m⁻² s⁻¹ from 05:00 until 12:00, with levels then remaining constant until around 16:00. There follows a steady decrease in NO₂ flux throughout the rest of the day and into the night, with levels reaching around 1200 ng m⁻² s⁻¹ at midnight.

Very few direct flux measurements of NO and NO₂ have been made in an urban environment, however the values measured in this study are comparable to those of a study in the urban area of Norfolk, VA, USA, which reported total NO_x fluxes in the range 5000–8000 ng m⁻² s⁻¹.³³ Direct measurements of NO_x fluxes have been made previously over forested and snowpack environments, with the measured fluxes still positive, but typically an order of magnitude smaller than measured here.^{22,24,25} Because of the close coupling of NO and NO₂, it is the sum NO_x that is typically reported in emission inventories, and so the rest of this work will concentrate on measurements of total NO_x. This also allows us to discount the chemistry associated with the interconversion of NO and NO₂, which can happen on a very fast time scale. Total NO_x is likely to be conserved between emission and sampling on the BT Tower, as formation of NO_x reservoir species such as PAN and HNO₃ takes place on a much longer time scale than the time between emission from street level and sampling at the tower (estimated as 3–8 min).

Analysis of the wind sector dependence of the flux can help to identify the sources of the species in question. Figure 1 shows bivariate polar plots with the joint flux footprint–wind direction of the NO_x flux, created using the Openair package.⁴⁶ The flux footprint used was calculated using the method described above. Two plots are shown to reflect daytime (05:00–19:00) and nighttime fluxes. During the daytime, there are clearly higher fluxes measured when the calculated footprint is smaller, in particular when the wind is from an E/NE direction from the tower. Fluxes then get smaller as the footprint gets larger in all directions. This is a reflection of the reduced traffic density (and hence traffic emissions), further away from central London. At night the fluxes are lower in all directions and for all footprints (as expected), however there is much less of a reduction in flux as the footprint gets larger. An explanation for this behavior is likely that traffic emissions are much less important for the total nighttime NO_x emission, with the majority of the emissions from commercial, industrial, and domestic combustion. Hence, there is more homogeneity over London during the night compared to the daytime. There are still greater fluxes measured when the wind was from the NE–SE sector, which is probably due to the area to the east of the tower being more urban in nature than that to the west.

Concentrations of a given pollutant in the atmosphere are largely dependent on its emission rate, meteorology, and chemical processing. It is useful to consider diurnal profiles in all these quantities because it can help understand the processes leading to what is observed. For diurnal averages, systematic uncertainties greatly outweigh random uncertainties which decrease as 1/√*n*, with *n* being the sample size. Average diurnal cycles have been calculated for the entire measurement period, for NO_x flux, average traffic volume at 20 traffic counting sites within the flux footprint of the site, boundary layer height, and

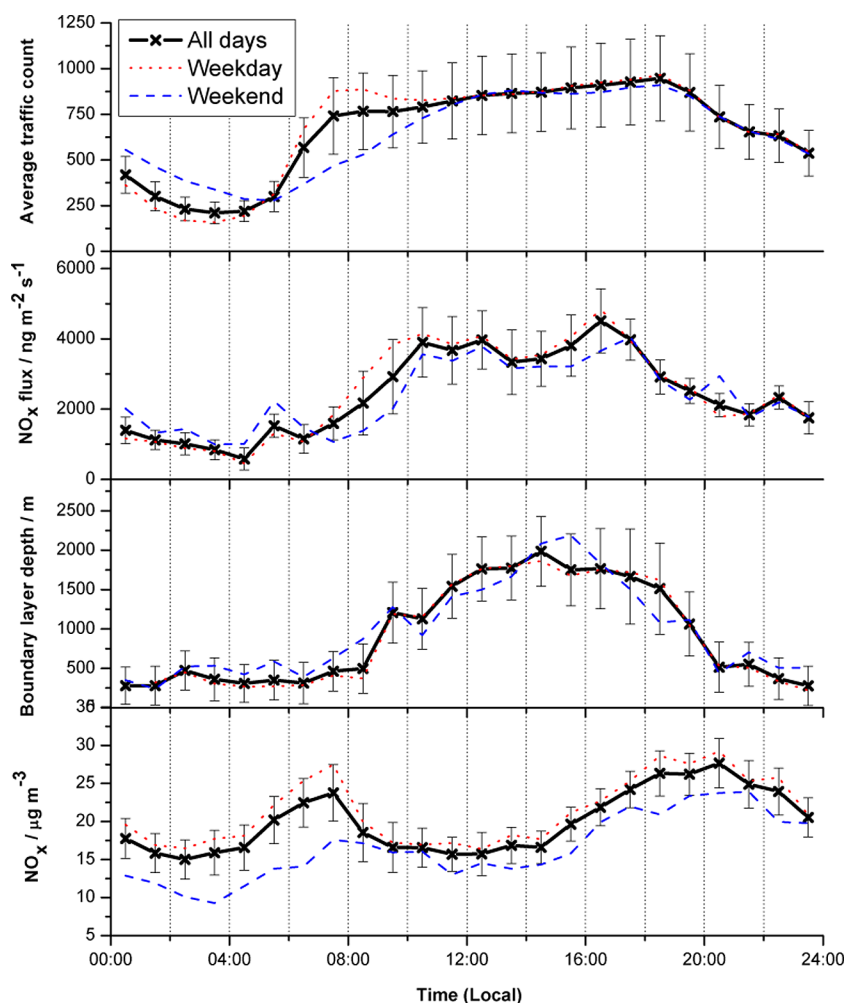


Figure 2. Average diurnal profiles for 36 days of data during Jun–Aug 2012 and 28 days during March–April 2013. Data shown are average traffic count (see text for further details), NO_x flux, boundary layer depth, and NO_x mass mixing ratio. All times are local time, with the time stamp being the midpoint of an hour averaging period. Error bars reflect the 95% confidence intervals in the mean of the different measurements used to calculate the diurnal average. The red dotted line shows weekday data and the blue dashed line shows weekend data.

NO_x concentration, and these data are shown in Figure 2 (all times local time). Standard deviations of the average diurnals are also shown, demonstrating the relatively small day to day variability of the measurements. The traffic data used can be thought of as a proxy for total traffic flow across the entire flux footprint area, and a map of the location of the traffic counting sites used is shown in the SI (Figure S5). Data from each day are binned into hourly time periods (local time – UTC + 1 h) and averaged, with the time stamp being the midtime of the averaging period. NO_x flux shows a diurnal cycle with positive fluxes seen throughout the day. From 00:00 to 04:00 fluxes are slightly decreasing from $1400 \pm 210 \text{ ng m}^{-2} \text{ s}^{-1}$ to $450 \pm 67 \text{ ng m}^{-2} \text{ s}^{-1}$, with a rise starting at around 04:30, consistent with the onset of the morning rush hour in London (at 05:30 local time). There follows a steady increase in the NO_x flux to around $4000 \pm 600 \text{ ng m}^{-2} \text{ s}^{-1}$ at 10:00, levels that remain until 17:00 (with a slight second peak at 16:00). This is broadly similar to the average traffic count data, providing more evidence that the majority of the NO_x emissions sampled at the BT Tower are from road traffic emissions. There then follows a steady decrease in the NO_x flux throughout the rest of the day, to around $1200 \pm 180 \text{ ng m}^{-2} \text{ s}^{-1}$ at 00:00. This is, again, broadly in line with the traffic flow. NO_x concentrations are reasonably stable at $\sim 18\text{--}20 \text{ } \mu\text{g m}^{-3}$ throughout the night,

followed by a rapid rise starting at 04:30 (at a time similar to the rise in NO_x flux). This rapid rise is due to a combination of the increase in fluxes, and the fact that the boundary layer height does not increase until around 06:30. Once the boundary layer starts to grow (from $\sim 300 \text{ m}$ at 08:00 to 1700 m at 12:00), the rise in NO_x concentrations is less rapid, and in fact they start to fall after a peak of $22 \text{ } \mu\text{g m}^{-3}$ at 08:00 until 16:00. This is likely due to dilution effects caused by the increasing height of the boundary layer, meaning the NO_x is emitted into a larger volume. After 15:30, the NO_x concentrations start to rise again, despite a decrease in flux. This is again likely due to the meteorology, with a decreasing boundary layer height into the night.

Also, plotted in Figure 2 are the weekday and weekend diurnal averages for the data. During the day, traffic counts are on average lower during the weekend, particularly during the morning where the difference is up to 50%. This is reflected in the NO_x flux data, although it does not show as pronounced a difference between weekend and weekday. This is potentially due to the type of traffic at the weekend, which is likely to be predominantly buses and larger vehicles (mainly powered by diesel engines), whereas during the week, private cars and taxis maybe more prevalent. During the night, traffic levels are actually higher on the weekend than during the day, also likely

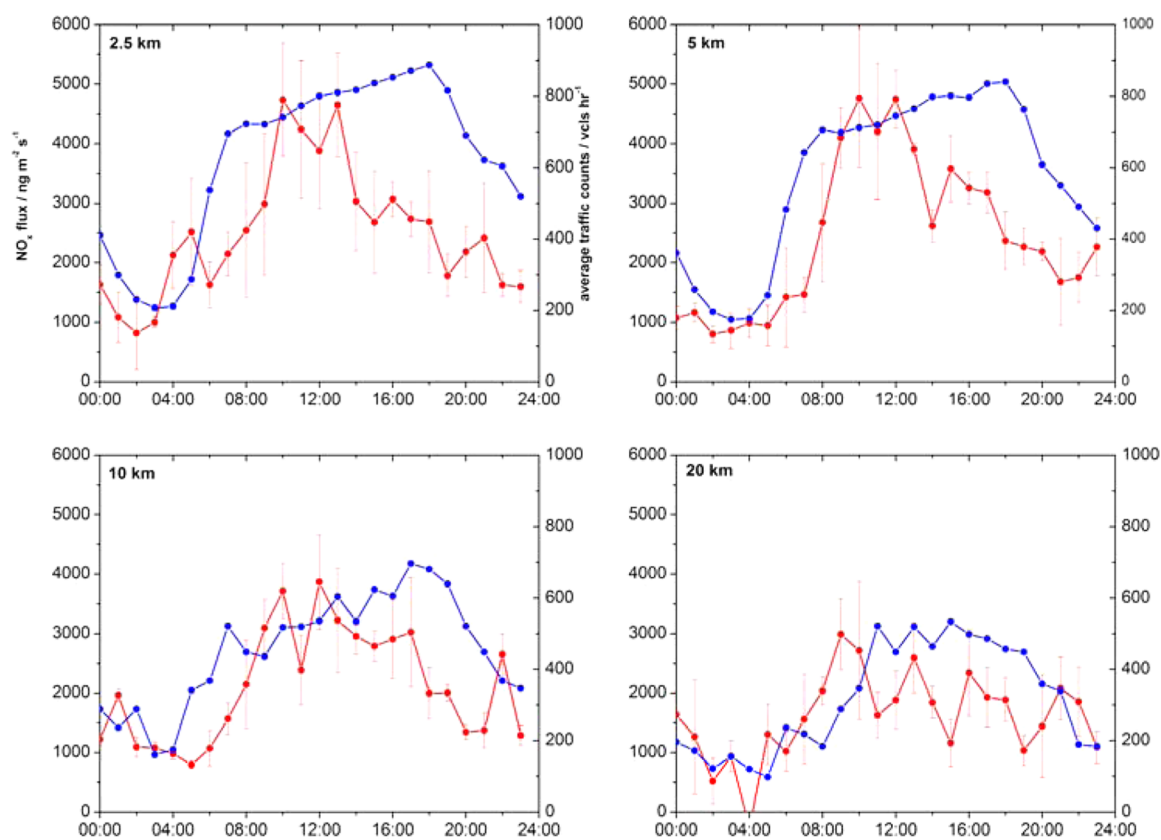


Figure 3. Average diurnal profiles for NO_x flux in 4 different footprint regimes (red trace). The error bars reflect the 95% confidence intervals in the mean of the different measurements used to calculate the diurnal average. All times are local time, with the time stamp being the midpoint of an hourly averaging period. Also shown is the average traffic flow at 6 sites within each of the individual footprint areas (blue trace).

to be a result of public transport and the large nighttime weekend economy of London. This is also reflected in the NO_x flux measurements showing higher values from midnight to 06:30 for weekends compared to weekdays.

The flux data were binned into 4 different regimes according to the calculated footprint (0–2.5, >2.5–5, >5–10, and >10–20 km radial distance from the BT Tower), and average diurnal profiles for each are plotted in Figure 3. The shaded regions represent the 95% confidence of the day to day variability of the flux measurements. All regimes show a similar diurnal profile, with the flux starting to rise at around 04:30, with a peak between 10:00 and 14:00. The highest fluxes are seen in the two smallest footprint regimes, with both showing similar values during daytime of around $4500 \pm 675 \text{ ng m}^{-2} \text{ s}^{-1}$. The 5–10 km regime shows lower daytime peak fluxes of $3200 \pm 480 \text{ ng m}^{-2} \text{ s}^{-1}$, with the 10–20 km regime lower still, with a peak of $2950 \pm 442 \text{ ng m}^{-2} \text{ s}^{-1}$ at 10:00 and then a decline throughout the day. All 4 regimes show similar NO_x fluxes at night of around $1000 \pm 150 \text{ ng m}^{-2} \text{ s}^{-1}$, the exception being the 0–2.5 km, which does exhibit some elevated flux levels up to $1500 \text{ ng m}^{-2} \text{ s}^{-1}$, and appears to start to rise slightly earlier than the other regimes. All this behavior is consistent with traffic emissions being the dominant source of NO_x , especially in central London. It is expected that traffic volume will be higher closer to central London and this is shown by the average traffic counts also plotted in the different footprint bins in Figure 4. As a result of this, the smaller footprint regimes from the BT Tower show the largest daytime fluxes. At night, it is likely that a smaller proportion of the NO_x will come from traffic sources,

meaning the measured flux will be similar in all flux regimes out to 20 km from the measurements site.

Emissions Inventories. To put the measured data in some context, a comparison has been carried out against inventories of NO_x emissions for London. The UK National Atmospheric Emissions Inventory (NAEI) shows official annual, spatially disaggregated, $1 \times 1 \text{ km}$ gridded emission maps for a wide range of atmospheric pollutants, including NO_x . A detailed description on how the emissions maps are produced is given in Bush et al.⁴⁷ Briefly, annual emission estimates are generated from 11 source sectors, according to those laid out by the United Nations Economic Commission for Europe (UNECE). For each sector, a national total emission estimate is produced from a combination of reported emissions and estimates based on modeling. The UK National Atmospheric Emission Inventory (NAEI) gives an estimate of the NO_x emissions in 1-km^2 grids over the UK, including a breakdown of the different sources. The NAEI estimate for NO_x emissions for London is shown in the SI (Figure S6). The map is centered on the BT Tower, and features of London characterized by large NO_x emissions can clearly be seen (e.g., Heathrow airport to the West and the M25 orbital motorway circling the city). Four maps are shown, with the contribution from 3 of the most important sectors (road transport; domestic, industrial, and commercial combustion; and other transport (rail and shipping)), as well as the total emissions. Also shown on the maps are 5-km and 10-km radius circles from the tower, indicative of the flux footprint bins described above. It suggests that around 65% of NO_x emissions from central London are from road and other transport, with the majority of the

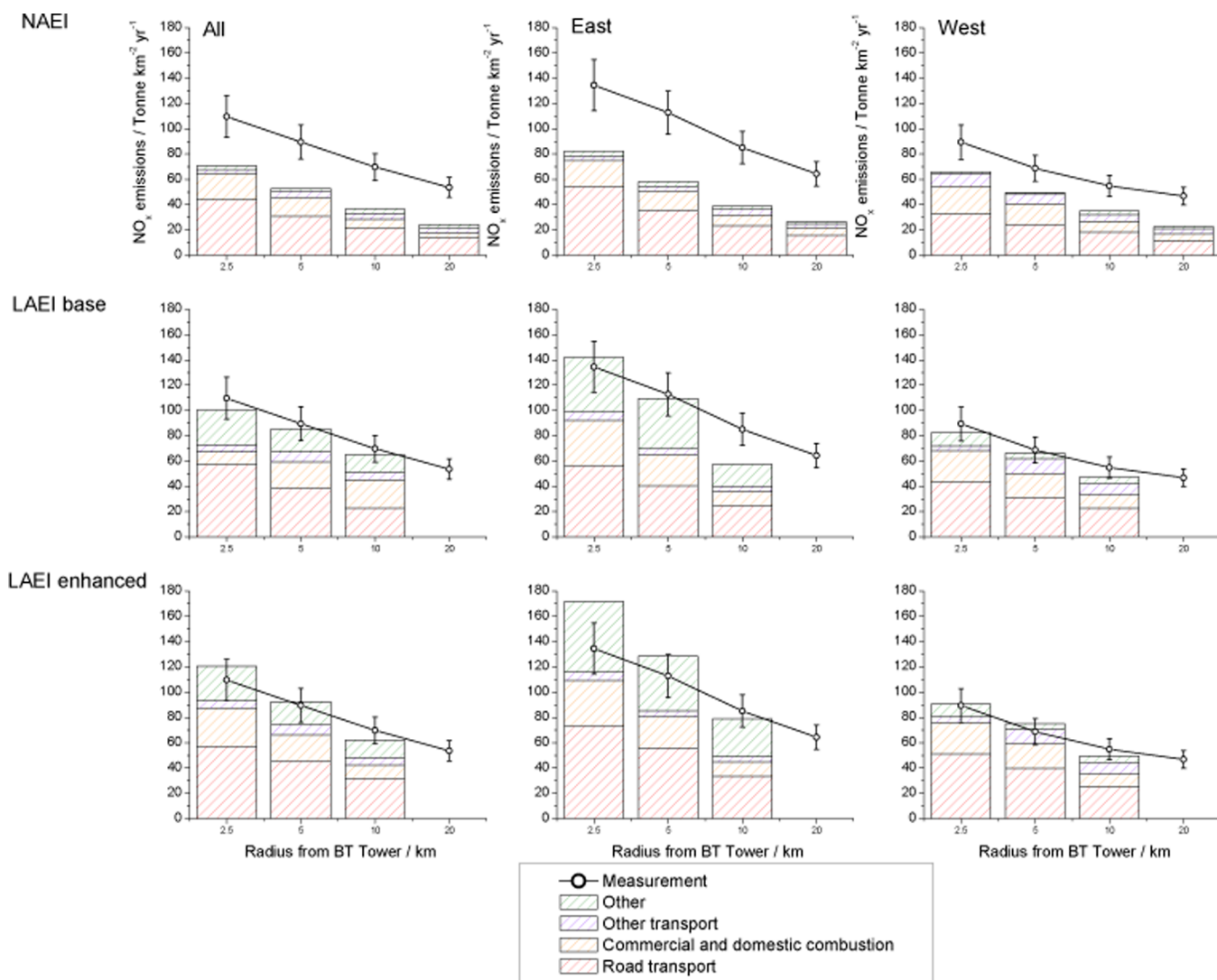


Figure 4. Comparison of the averaged measured fluxes, scaled to give an annual emission rate, with the estimate of the National Atmospheric Emission Inventory (NAEI) and two versions of the London Atmospheric Emissions Inventory (LAEI); see text for details. The different colors in the columns represent the estimates from different source sectors.

remainder from commercial, domestic, and industrial combustion.

The London Atmospheric Emissions Inventory (LAEI) provides emissions estimates of 9 air pollutants (including NO_x), on a 20 m × 20 m grid square scale. The inventory reflects the geography of the roads in London, enabling an accurate assessment of population exposure and health impacts. Two versions of the LAEI are used in this study. The standard LAEI (LAEI base) is the 2012 inventory based on methods set out in the Greater London Authority datastore,⁴⁸ but updated for 2012 emission data. Also, we use an enhanced version of the LAEI, which uses measured roadside emissions based on extensive vehicle emission remote sensing.⁴⁹ Both emissions inventories discussed are purely annual averages with no seasonal or finer temporal detail.

Comparison with Measurements. Figure 4 shows estimated emissions of NO_x taken from the NAEI and LAEI for 2.5-, 5-, and 10-km radial distance from the tower, along with the estimates for sections in easterly (30–150°) and westerly (210–330°) directions and the source sector estimate divided into road transport, commercial and residential

combustion, and other transport (which is mainly rail in London). For the NAEI data for a 20-km radial distance is also plotted, however this data is not available for the LAEI. Also plotted is the averaged measured NO_x flux for the different footprint regimes, also divided into periods of easterly and westerly wind directions and scaled to give a yearly emission rate.

The measurements are seen to be significantly higher than those of the NAEI (outside the estimated experimental flux systematic error of 15%) under all regimes. The agreement between the measurement and the inventory tends to get worse for the larger footprint regimes, with the measurement being 2.2 times higher than the inventory for the 10–20 km regime, and only 1.6 times higher for the 0–2.5 km regime. There is much more scope for error when considering a comparison between larger flux footprints and the inventory, as the further the air has traveled, the more different emission inventory grid squares it could have passed over, making a comparison with the inventory more difficult. In general, the agreement is better for the westerly flow conditions, with the measurement being 1.36 and 1.38 times higher than the inventory for the 2.5- and

5-km footprints, respectively, whereas for the easterly flow, the agreement is worse (1.6 and 1.9 times higher for 2.5 and 5 km). The difference in source sector between the 2.5- and 5-km radius is small. Road transport dominates (62% and 60% for 2.5 and 5 km, respectively), with the remainder from commercial and domestic combustion (29% and 27%) and other transport (4% and 10%). There is a lower contribution from road transport for the westerly flow conditions (48% for both 2.5- and 5-km radius), giving a potential reason for the better agreement here. It is likely that road transport is the most poorly constrained part of the NAEI, and hence when this is less important to the total emission rate, the agreement with the measurement is better.

For the base LAEI, the comparison shows a much closer agreement of the measurements with the inventory compared to that with the NAEI discussed above. The inventory is within the measurement error for the average of all wind directions, with the measurement 1.03 and 1.1 times higher than the inventory in the 2.5- and 5-km regimes, respectively. The agreement is similarly good in westerly flow, and although in easterly flow the measurement is now 1.07 times lower for the 2.5-km footprint and 1.03 times higher for the 5-km footprint, these are still well within measurement error. For the 10-km footprint, the LAEI falls outside the systematic error of the measurements for all the data separated into easterly and westerly flow regimes, with the measurements being 1.16 and 1.48 times higher than the inventory for westerly and easterly flow, respectively. A comparison of the measurements to the enhanced LAEI (which has generally increased road transport NO_x emissions), shows the measurements being slightly lower than the inventory for data from the 2.5- and 5-km flux footprints, although again these are still within the systematic error of the measurements for all the data and the westerly flow. It is in the easterly flow conditions where the measurements are now significantly lower than the inventory, with the underestimation of 20% and 17% for the 2.5- and 5-km regimes falling outside the flux measurement error. For the 10-km flux footprint regime, the enhanced LAEI brings the emission estimates into much better agreement with the measurements than the base case, with the data from both easterly and westerly flows showing agreement within 10%.

In general, both the LAEIs seem to be doing a reasonable job of estimating NO_x emissions in central London, and certainly better than the NAEI estimations. The LAEI, particularly in its enhanced form with measured road traffic emissions, has a much more explicit treatment of road transport emission than the NAEI, thus potentially providing a more accurate estimate of NO_x emissions in London. It uses vehicle speed and vehicle flow data from each road link using GPS-based vehicle speed, and automatic number plate recognition data to enhance vehicle stock information. The inventory also makes predictions of primary NO_2 emissions, something that is potentially important in London due to the high proportion of diesel-fueled vehicles, which are likely to have a higher direct primary NO_2 emission compared to gasoline vehicles.⁵⁰ The LAEI containing the enhanced treatment of traffic emissions actually overestimates the NO_x emission in the central London footprint regimes (0–5 km from the BT Tower), with greater overestimation outside the error of the measurements under easterly flow conditions. This suggests potential extra errors in the treatment of traffic flow in the center of London to the east of the BT Tower within the LAEI. The LAEI has a significant contribution from other sources, which are mainly from

nonroad mobile machinery (e.g., cranes, construction vehicles). These are virtually zero in the NAEI and it could be errors in these sources that are contributing to the overestimation of the inventory in central London. The better comparison with the LAEI compared to the NAEI supports previous tailpipe observations of higher NO_x emitted from the London vehicle diesel fleet than is represented in the NAEI or predicted for several EURO emission control technologies, and shows that a detailed treatment of traffic emissions is required to properly predict the NO_x emissions.¹¹ There are no studies to our knowledge that specifically evaluate the London or national inventories. However, it is clear from recent remote sensing measurements in London during 2012 that emissions of NO_x have not decreased as expected through emissions legislation.⁴⁹ This higher-than-anticipated vehicle NO_x is likely responsible for the significant discrepancies that exist in London between observed NO_x and long-term NO_x projections, and show that a detailed representation of traffic emissions is required to accurately represent NO_x in London.

■ ASSOCIATED CONTENT

📄 Supporting Information

Figures S1–S6: a location map of the site, the time series of NO_x levels and fluxes from the BT Tower, regression between BT Tower NO_x and NO_x measured at a nearby urban background site, flux footprint statistics, a map of the location of the traffic count sites, and maps of the 1 km × 1 km National Atmospheric Emission Inventory (NAEI) source-specific emissions for NO_x . This material is available free of charge via the Internet at <http://pubs.acs.org/>

■ AUTHOR INFORMATION

Corresponding Author

* Phone: +44 0 1904 322575; e-mail: james.lee@york.ac.uk.

Notes

The authors declare no competing financial interest.

■ ACKNOWLEDGMENTS

We thank BT, in particular Robert Semon, Karen Ahern, and Andy Beale for their support in granting access to the BT Tower for the measurements and logistical help in setting up the instrumentation. Thanks go to Janet Barlow and Christoforos Halios for provision of the fast time meteorological and boundary layer data at the BT Tower. The work was funded through the UK Natural Environment Research Council (NERC) ClearLo project (grant NE/H00324X/1).

■ REFERENCES

- (1) Tunnicliffe, W. S.; Burge, P. S.; Ayres, J. G. Effect of domestic concentrations of nitrogen dioxide on airway responses to inhaled allergen in asthmatic patients. *Lancet* **1994**, *344* (8939–4), 1733–1736.
- (2) Strand, V.; Svartengren, M.; Rak, S.; Barck, C.; Bylin, G. Repeated exposure to an ambient level of NO_2 enhances asthmatic response to a nonsymptomatic allergen dose. *Eur. Respir. J.* **1998**, *12* (1), 6–12.
- (3) Logan, J. A.; Prather, M. J.; Wofsy, S. C.; McElroy, M. B. Tropospheric Chemistry - A Global Perspective. *J. Geophys. Res.* **1981**, *86* (NC8), 7210–7254.
- (4) AQD. Directive 2008/50/EC of the European Parliament and of the Council of 21 May 2008 on ambient air quality and cleaner air for Europe; 2008.
- (5) Brookes, D. M.; Stedman, J. R.; Kent, A. J.; King, R. J.; Venfield, H. L.; Cooke, S. L.; Lingard, J. J. N.; Vincent, K. J.; Bush, T. J.; Abbott, J. *Technical Report on UK Supplementary Assessment under the Air*

Quality Directive (2008/50/EC), the Air Quality Framework Directive (96/62/EC) and Fourth Daughter Directive (2004/107/EC) for 2011; Ricardo-AEA report AEAT/ENV/R/3316; Defra: London, 2012.

(6) Misra, A.; Passant, N. R.; Murrells, T. P.; Thistlethwaite, G.; Pang, Y.; BNorris, J.; Walker, C.; Stewart, R. A.; MacCarthy, J.; Pierce, M., *UK Emission Projections of Air Quality Pollutants to 2030*; AEA Technology report AEA/ENV/R/3337, 2012. [http://uk-air.defra.gov.uk/reports/cat07/1211071420_UEP43_\(2009\)_Projections_Final.pdf](http://uk-air.defra.gov.uk/reports/cat07/1211071420_UEP43_(2009)_Projections_Final.pdf).

(7) Derwent, R. G.; Middleton, D. R.; Field, R. A.; Goldstone, M. E.; Lester, J. N.; Perry, R. Analysis and interpretation of air quality data from an urban roadside location in central London over the period July 1991 to July 1992. *Atmos. Environ.* **1995**, *29* (8), 923–946.

(8) Sillman, S. The relation between ozone, NO_x and hydrocarbons in urban and polluted rural environments. *Atmos. Environ.* **1999**, *33* (12), 1821–1845.

(9) Carslaw, D. C. Evidence of an increasing NO₂/NO_x emissions ratio from road traffic emissions. *Atmos. Environ.* **2005**, *39* (26), 4793–4802.

(10) Beevers, S. D.; Westmoreland, E.; de Jong, M. C.; Williams, M. L.; Carslaw, D. C. Trends in NO_x and NO₂ emissions from road traffic in Great Britain. *Atmos. Environ.* **2012**, *54*, 107–116.

(11) Carslaw, D. C.; Beevers, S. D.; Tate, J. E.; Westmoreland, E. J.; Williams, M. L. Recent evidence concerning higher NO_x emissions from passenger cars and light duty vehicles. *Atmos. Environ.* **2011**, *45* (39), 7053–7063.

(12) Simon, H.; Allen, D. T.; Wittig, A. E. Fine particulate matter emissions inventories: Comparisons of emissions estimates with observations from recent field programs. *J. Air Waste Manage. Assoc.* **2008**, *58* (2), 320–343.

(13) Han, K. M.; Song, C. H.; Ahn, H. J.; Park, R. S.; Woo, J. H.; Lee, C. K.; Richter, A.; Burrows, J. P.; Kim, J. Y.; Hong, J. H. Investigation of NO_x emissions and NO_x-related chemistry in East Asia using CMAQ-predicted and GOME-derived NO₂ columns. *Atmos. Chem. Phys.* **2009**, *9* (3), 1017–1036.

(14) Ying, Q.; Lu, J.; Allen, P.; Livingstone, P.; Kaduwela, A.; Kleeman, M. Modeling air quality during the California Regional PM10/PM2.5 Air Quality Study (CRPAQS) using the UCD/CIT source-oriented air quality model - Part I. Base case model results. *Atmos. Environ.* **2008**, *42* (39), 8954–8966.

(15) Lee, X.; Massman, W.; Law, B. *Handbook of Micrometeorology: A Guide for Surface Flux Measurement and Analysis*; Kluwer Academic Publishers: Dordrecht, The Netherlands, 2004.

(16) Moore, T. O.; Doughty, D. C.; Marr, L. C. Demonstration of a mobile Flux Laboratory for the Atmospheric Measurement of Emissions (FLAME) to assess emissions inventories. *J. Environ. Monit.* **2009**, *11* (2), 259–268.

(17) Aubinet, M.; Chermanne, B.; Vandenhaute, M.; Longdoz, B.; Yernaux, M.; Laitat, E. Long term carbon dioxide exchange above a mixed forest in the Belgian Ardennes. *Agric. For. Meteorol.* **2001**, *108* (4), 293–315.

(18) Davison, B.; Taipale, R.; Langford, B.; Misztal, P.; Fares, S.; Matteucci, G.; Loreto, F.; Cape, J. N.; Rinne, J.; Hewitt, C. N. Concentrations and fluxes of biogenic volatile organic compounds above a Mediterranean macchia ecosystem in western Italy. *Biogeosciences* **2009**, *6* (8), 1655–1670.

(19) Lee, A.; Schade, G. W.; Holzinger, R.; Goldstein, A. H. A comparison of new measurements of total monoterpene flux with improved measurements of speciated monoterpene flux. *Atmos. Chem. Phys.* **2005**, *5*, 505–513.

(20) Karl, T.; Guenther, A.; Lindinger, C.; Jordan, A.; Fall, R.; Lindinger, W. Eddy covariance measurements of oxygenated volatile organic compound fluxes from crop harvesting using a redesigned proton-transfer-reaction mass spectrometer. *J. Geophys. Res.* **2001**, *106* (D20), 24157–24167.

(21) Stella, P.; Loubet, B.; Laville, P.; Lamaud, E.; Cazaunau, M.; Laufs, S.; Bernard, F.; Grosselin, B.; Mascher, N.; Kurtenbach, R.; Mellouki, A.; Kleffmann, J.; Cellier, P. Comparison of methods for the

determination of NO-O₃-NO₂ fluxes and chemical interactions over a bare soil. *Atmos. Meas. Technol.* **2012**, *5* (6), 1241–1257.

(22) Min, K. E.; Pusede, S. E.; Browne, E. C.; LaFranchi, B. W.; Wooldridge, P. J.; Cohen, R. C. Eddy covariance fluxes and vertical concentration gradient measurements of NO and NO₂ over a ponderosa pine ecosystem: observational evidence for within-canopy chemical removal of NO_x. *Atmos. Chem. Phys.* **2014**, *14* (11), 5495–5512.

(23) Geddes, J. A.; Murphy, J. G. Observations of reactive nitrogen oxide fluxes by eddy covariance above two midlatitude North American mixed hardwood forests. *Atmos. Chem. Phys.* **2014**, *14* (6), 2939–2957.

(24) Rummel, U.; Ammann, C.; Gut, A.; Meixner, F. X.; Andreae, M. O. Eddy covariance measurements of nitric oxide flux within an Amazonian rain forest. *J. Geophys. Res.* **2002**, *107* (D20), LBA 17-1–LBA 17-9.

(25) Honrath, R. E.; Lu, Y.; Peterson, M. C.; Dibb, J. E.; Arsenualt, M. A.; Cullen, N. J.; Steffen, K. Vertical fluxes of NO_x, HONO, and HNO₃ above the snowpack at Summit, Greenland. *Atmos. Environ.* **2002**, *36* (15–16), 2629–2640.

(26) Bakwin, P. S.; Wofsy, S. C.; Fan, S. M.; Fitzjarrald, D. R. Measurements of NO_x and NO_y Concentrations and Fluxes Over Arctic Tundra. *J. Geophys. Res.* **1992**, *97* (D15), 16545–16557.

(27) Velasco, E.; Pressley, S.; Allwine, E.; Westberg, H.; Lamb, B. Measurements of CO₂ fluxes from the Mexico City urban landscape. *Atmos. Environ.* **2005**, *39* (38), 7433–7446.

(28) Vesala, T.; Jarvi, L.; Launiainen, S.; Sogachev, A.; Rannik, U.; Mammarella, I.; Siivola, E.; Keronen, P.; Rinne, J.; Riikonen, A.; Nikinmaa, E. Surface-atmosphere interactions over complex urban terrain in Helsinki, Finland. *Tellus B* **2008**, *60* (2), 188–199.

(29) Crawford, B.; Grimmond, C. S. B.; Christen, A. Five years of carbon dioxide fluxes measurements in a highly vegetated suburban area. *Atmos. Environ.* **2011**, *45* (4), 896–905.

(30) Langford, B.; Nemitz, E.; House, E.; Phillips, G. J.; Famulari, D.; Davison, B.; Hopkins, J. R.; Lewis, A. C.; Hewitt, C. N. Fluxes and concentrations of volatile organic compounds above central London, UK. *Atmos. Chem. Phys.* **2010**, *10* (2), 627–645.

(31) Langford, B.; Davison, B.; Nemitz, E.; Hewitt, C. N. Mixing ratios and eddy covariance flux measurements of volatile organic compounds from an urban canopy (Manchester, UK). *Atmos. Chem. Phys.* **2009**, *9* (6), 1971–1987.

(32) Velasco, E.; Lamb, B.; Pressley, S.; Allwine, E.; Westberg, H.; Jobson, B. T.; Alexander, M.; Prazeller, P.; Molina, L.; Molina, M. Flux measurements of volatile organic compounds from an urban landscape. *Geophys. Res. Lett.* **2005**, *32* (20), No. L20802.

(33) Marr, L. C.; Moore, T. O.; Klappmeyer, M. E.; Killar, M. B. Comparison of NO_x fluxes measured by eddy covariance to emission inventories and land use. *Environ. Sci. Technol.* **2013**, *47* (4), 1800–1808.

(34) Bohnenstengel, S. I.; Belcher, S. E.; Aiken, A.; Allan, J. D.; Allen, G.; Bacak, A.; Bannan, T. J.; Barlow, J. F.; Beddows, D. C. S.; Bloss, W. J.; Booth, A. M.; Chemel, C.; Coceal, O.; Di Marco, C. F.; Dube, M. K.; Faloon, K. H.; Fleming, Z. L.; Furger, M.; Gietl, J. K.; Graves, R. R.; Green, D. C.; Grimmond, C. S. B.; Halios, C. H.; Hamilton, J. F.; Harrison, R. M.; Heal, M. R.; Heard, D. E.; Helfter, C.; Herndon, S. C.; Holmes, R. E.; Hopkins, J. R.; Jones, A. M.; Kelly, F. J.; Kotthaus, S.; Langford, B.; Lee, J. D.; Leigh, R. J.; Lewis, A. C.; Lidster, R. T.; Lopez-Hilfiker, F. D.; McQuaid, J. B.; Mohr, C.; Monks, P. S.; Nemitz, E.; Ng, N. L.; Percival, C. J.; Prévôt, A. S. H.; Ricketts, H. M. A.; Sokhi, R.; Stone, D.; Thornton, J. A.; Tremper, A. H.; Valach, A. C.; Visser, S.; Whalley, L. K.; Williams, L. R.; Xu, L.; Young, D. E.; Zotter, P. Meteorology, air quality, and health in London: The ClearLo project. *Bull. Am. Meteorol. Soc.* **2014**, No. 10.1175/BAMS-D-12-00245.1.

(35) Helfter, C.; Famulari, D.; Phillips, G. J.; Barlow, J. F.; Wood, C. R.; Grimmond, C. S. B.; Nemitz, E. Controls of carbon dioxide concentrations and fluxes above central London. *Atmos. Chem. Phys.* **2011**, *11* (5), 1913–1928.

- (36) Dickerson, R. R.; Delany, A. C.; Wartburg, A. F. Further modification of a commercial NO_x detector for high sensitivity. *Rev. Sci. Instrum.* **1984**, *55* (12), 1995–1998.
- (37) Lee, J. D.; Moller, S. J.; Read, K. A.; Lewis, A. C.; Mendes, L.; Carpenter, L. J. Year-round measurements of nitrogen oxides and ozone in the tropical North Atlantic marine boundary layer. *J. Geophys. Res.* **2009**, *114*, No. D21302.
- (38) Pollack, I. B.; Lerner, B. M.; Ryerson, T. B. Evaluation of ultraviolet light-emitting diodes for detection of atmospheric NO₂ by photolysis - chemiluminescence. *J. Atmos. Chem.* **2010**, *65* (2–3), 111–125.
- (39) Barlow, J. F.; Dunbar, T. M.; Nemitz, E. G.; Wood, C. R.; Gallagher, M. W.; Davies, F.; O'Connor, E.; Harrison, R. M. Boundary layer dynamics over London, UK, as observed using Doppler lidar during REPARTEE-II. *Atmos. Chem. Phys.* **2011**, *11* (5), 2111–2125.
- (40) Foken, T.; Wichura, B. Tools for quality assessment of surface-based flux measurements. *Agric. For. Meteorol.* **1996**, *78* (1–2), 83–105.
- (41) Foken, T.; Godecke, M.; Mauder, M.; Mahrt, L.; Amiro, B.; Munger, W. Post-field data quality control. In *Handbook of Micrometeorology*; Lee, X., Ed. Kluwer Academic Publishers: Dordrecht, The Netherlands, 2004.
- (42) Hollinger, D. Y.; Richardson, A. D. Uncertainty in eddy covariance measurements and its application to physiological models. *Tree Physiol.* **2005**, *25* (7), 873–885.
- (43) Kormann, R.; Meixner, F. X. An analytical footprint model for non-neutral stratification. *Bound.-Layer Meteorol.* **2001**, *99* (2), 207–224.
- (44) Bigi, A.; Harrison, R. M. Analysis of the air pollution climate at a central urban background site. *Atmos. Environ.* **2010**, *44* (16), 2004–2012.
- (45) Wesely, M. L.; Hicks, B. B. A review of the current status of knowledge on dry deposition. *Atmos. Environ.* **2000**, *34* (12–14), 2261–2282.
- (46) Carslaw, D. C.; Ropkins, K. openair - An R package for air quality data analysis. *Environ. Modell. Softw.* **2012**, *27–28*, 52–61.
- (47) Bush, T. J.; Tsagatakis, I.; King, K.; Passant, N. R. *NAEI UK Emission Mapping Methodology 2006*. AEATY/ENV/R/2696; 2006; <http://www.naei.org.uk/reoprts.php>.
- (48) Greater London Authority – London Datastore. <http://data.london.gov.uk/>.
- (49) Carslaw, D. C.; Rhys-Tyler, G. New insights from comprehensive on-road measurements of NO_x, NO₂ and NH₃ from vehicle emission remote sensing in London, UK. *Atmos. Environ.* **2013**, *81*, 339–347.
- (50) Carslaw, D. C.; Beevers, S. D. Investigating the potential importance of primary NO₂ emissions in a street canyon. *Atmos. Environ.* **2004**, *38* (22), 3585–3594.